DMD Fast Forward. Published on January 13, 2006 as doi:10.1124/dmd.105.008508

DMD #8508

Stereochemical Aspects of Itraconazole Metabolism in vitro and in vivo

Kent L Kunze, Wendel L Nelson, Evan D Kharasch, Kenneth E Thummel and Nina Isoherranen

From the Department of Pharmaceutics (NI and KET) and Department of Medicinal Chemistry (KLK, WLN and EDK), School of Pharmacy and Department of Anesthesiology (EDK), School of Medicine, University of Washington, Seattle

Running title: Itraconazole stereoselective metabolism

Corresponding Author:

Correspondence: Dr. Nina Isoherranen, Department of Pharmaceutics, H272 Health Sciences Building, Box 357610, University of Washington, Seattle, WA 98195, USA.
Tel.: +1 206 543 2517; fax: +1 206 543 3204
e-mail: ni2@u.washington.edu

25 text pages

4 tables

6 figures

22 references

249 words in Abstract

771 words in Introduction

1485 words in Discussion

Nonstandard abbreviations used:

ITZ, itraconazole; OH-ITZ, hydroxy-itraconazole; Keto-ITZ, keto-itraconazole; ND-ITZ, N-desalkyl-itraconazole; CYP, cytochrome P450, Cl_{int}, intrinsic clearance; Kpi, Potassium phosphate

ABSTRACT

Itraconazole (ITZ) has three chiral centers and is administered clinically as a mixture of four stereoisomers. This study evaluated stereoselectivity in ITZ metabolism. In vitro experiments were carried out using heterologously expressed CYP3A4. Only (2R,4S,2'R)-ITZ and (2R,4S,2'S)-ITZ were metabolized by CYP3A4 to hydroxy-ITZ, keto-ITZ and N-desalkyl-ITZ. When (2S,4R,2'R)-ITZ or (2S,4R,2'S)-ITZ was incubated with CYP3A4, neither metabolites nor substrate depletion were detected. Despite these differences in metabolism, all four ITZ stereoisomers induced a type II binding spectrum with CYP3A4, characteristic of co-ordination of the triazole nitrogen to the heme iron (K_d 2.2-10.6 nM). All four stereoisomers of ITZ inhibited the CYP3A4-catalyzed hydroxylation of midazolam with high affinity (IC_{50} 3.7-14.8 nM). Stereochemical aspects of ITZ pharmacokinetics were evaluated in six healthy volunteers following single and multiple oral doses. In vivo, after single dose ITZ disposition was stereoselective, with a 3-fold difference in C_{max} and 9-fold difference in C_{min} between the (2R,4S)-ITZ and the (2S,4R)-ITZ pairs of diastereomers, with the latter reaching higher concentrations. Secondary and tertiary ITZ metabolites (keto-ITZ and N-desalkyl-ITZ) detected in plasma were of the (2R,4S) stereochemistry. After multiple doses of ITZ, the difference in C_{max} and C_{min} decreased to 1.5 and 3.8-fold, respectively. The initial difference between the stereoisomeric pairs was most likely due to stereoselective metabolism by CYP3A4 including stereoselective first pass metabolism as well as stereoselective elimination. However, stereoselective elimination was diminished after multiple dosing, presumably as a result of CYP3A4 auto-inhibition. In conclusion, the metabolism of ITZ is highly stereoselective in vitro and in vivo.

Itraconazole (ITZ) is a broad-spectrum triazole antifungal agent mainly used to treat infections caused by mixed dermatophyte and candida (Haria et al., 1996). It is also used for prophylaxis in patients with immunodepression (Poirier and Cheymol., 1998). The antifungal activity of ITZ is due to inhibition of the fungal cytochrome P450, 14α-demethylase, thus impairing the synthesis of ergosterol.

The ITZ molecule has three chiral centers (Figure 1). The two chiral centers in the dioxolane ring are fixed in relation to one another and the triazolomethylene and aryloxymethylene dioxolane-ring substituents are always cis to each other. The clinical formulation is a mixture of four stereoisomers (two enantiomeric pairs, Figure 1). ITZ stereoisomers with (2S,4R) configuration in the dioxolane ring ((2S,4R)-ITZ) are four-fold more potent in vitro against *Candida albicans* than those with the (2R,4S) configuration ((2R,4S)-ITZ) (Koch et al., 2000), but any studies assessing the antifungal activity of individual ITZ stereoisomers are unpublished.

Despite stereoselective differences in antifungal activity, the metabolism and disposition of ITZ stereoisomers are poorly understood. An electropherogram of a single plasma sample from one patient indicated differences in ITZ stereoisomer concentrations and results from an in vitro incubation suggested that ITZ metabolism may be stereoselective (Breadmore and Thormann., 2003). However, only two component peaks of ITZ were resolved, their absolute stereochemistry was not identified, and no pharmacokinetic or enzyme kinetic analysis was conducted. The prospect that stereochemistry may be a major determinant of antifungal activity, pharmacokinetics, and the magnitude of drug-drug interactions suggests that a single stereoisomer of ITZ might be clinically superior to the mixture of ITZ stereoisomers that is currently administered.

The achiral pharmacokinetics of the unresolved mixture of ITZ stereoisomers has been well characterized. ITZ has a large volume of distribution (11 l/kg), an intermediate hepatic extraction ratio (0.55) and dose- and time-dependent pharmacokinetics which are best described using a three-compartment model (Poirier and Cheymol, 1998; Haria et al., 1996). Following the rapid distribution phase, the slow distribution phase and the elimination phase might reflect the rapid and slow metabolism of stereoisomer pairs. Such stereoselective kinetics have been demonstrated by simulations (Tucker and Lennard, 1990) and reported previously for several drugs, including mephenytoin and warfarin (Levy and Boddy, 1991; Wedlund et al., 1985; Hutt and Tan, 1996).

ITZ is metabolized by CYP3A4 sequentially to three metabolites (Figure 2), OH-ITZ, keto-ITZ and N-desalkyl-ITZ (ND-ITZ) (Isoherranen et al., 2004) which are all present in plasma following administration of ITZ (Isoherranen et al. unpublished observations). Because keto-ITZ and ND-ITZ are formed sequentially from ITZ via OH-ITZ, it was suggested that the keto-ITZ and ND-ITZ observed in plasma would have identical stereochemical composition as the ITZ stereoisomers that are metabolized to OH-ITZ. Only CYP3A4 forms OH-ITZ from ITZ in vitro (Isoherranen et al., 2004) and clinically CYP3A4-catalyzed processes appear to make up a major elimination pathway for ITZ (Ducharme et al., 1995). Of the circulating metabolites, the pharmacokinetics of OH-ITZ has been best characterized. The half-life of OH-ITZ has been consistently described to be shorter than that of ITZ (Barone et al., 1993; Ducharme et al., 1995; Heykants et al., 1989), which is inconsistent with conventional pharmacokinetic theory. To explain this unusual behavior, it was hypothesized that formation of OH-ITZ is stereoselective. The ITZ stereoisomers that are converted to OH-ITZ would have a short half-life (the half-life of the α-phase of ITZ elimination) equivalent to or shorter than the half-life of OH-ITZ. The

clinically observed terminal half-life of ITZ would correspond to the elimination of stereoisomer(s) of ITZ that is (are) not metabolized by CYP3A4 to OH-ITZ or is (are) metabolized at a much slower rate.

ITZ is a potent inhibitor of CYP3A4 and causes significant drug-drug interactions when co-administered with other CYP3A4 substrates (Neuvonen et al., 1998; Olkkola et al., 1996; Backman et al., 1998; Florea et al., 2003; Mahnke et al., 2003). The mixture of stereoisomers of OH-ITZ, keto-ITZ and ND-ITZ are also potent inhibitors of CYP3A4 in vitro, and thus they may contribute to the inhibition of CYP3A4 observed in clinical situations (Isoherranen et al., 2004). The magnitude of the in vivo interactions observed with ITZ is greater than that predicted from in vitro data when reversible inhibition is assumed. Several reasons have been offered to explain the in vitro-in vivo discrepancy, including non-specific protein binding, selective uptake of ITZ into hepatocytes, and inhibitory metabolites of ITZ (Yamano et al., 1999; Yamano et al., 2001; Isoherranen et al., 2004). Stereoselective elimination of ITZ and its metabolites, together with CYP3A4 inhibition by stereoisomers of ITZ or the metabolites, may all contribute to the poor prediction of CYP3A4 inhibition in vivo.

The goals of this study were to determine whether the metabolism of ITZ by CYP3A4 and the inhibition of CYP3A4 by ITZ are stereoselective, and investigate the stereoselective disposition of itraconazole in vivo. To address these aims, the four ITZ stereoisomers were incubated with heterologously expressed CYP3A4, and ITZ depletion as well as formation of metabolites was measured. The IC_{50} values of the stereoisomers of ITZ were determined, and spectral titrations of ITZ stereoisomers with CYP3A4 were performed in order to obtain K_s-values. In addition, the stereoselective pharmacokinetic behavior of ITZ was studied in six healthy volunteers during administration of ITZ for seven days.

MATERIALS AND METHODS

Chemicals, Recombinant CYPs and human liver microsomes The four ITZ stereoisomers and four of the eight possible OH-ITZ stereoisomers (2R,4S,2'S,3'R)-OH-ITZ, (2R,4S,2'R,3'S)-OH-ITZ, (2R,4S,2'S,3'S)-OH-ITZ and (2R,4S,2'R,3'R)-OH-ITZ were obtained from Sepracor Inc (Marlborough, MA). The mixtures of ITZ and OH-ITZ stereoisomers were purchased from Research Diagnostics Inc, (Flanders, NJ). Keto-itraconazole was generously provided by Dr. Jan Heeres, Janssen Pharmaceutica N. V., Beerse, Belgium, and ND-ITZ was prepared as previously reported (Heeres et al., 1984; Isoherranen et al., 2004). Midazolam, 1′-hydroxymidazolam (OH-MDZ) and 1′-[$^2H_2$]-hydroxymidazolam were gifts from Roche Laboratories (Nutley, NJ). Acetonitrile was purchased from Fischer Scientific Co. (Fairlawn, NJ), ammonium acetate from J.T. Baker (Phillipsburg, NJ) and NADPH from Sigma-Aldrich (St. Louis, MO). Ultrapure water, filtered through a Barnstead Nanopure filter system, was used throughout the study.

Supersomes^{TM} containing cDNA-expressed CYP3A4 co-expressed with P450 reductase and cytochrome b_5 were purchased from BD Gentest Corp. (Woburn, MA). Purified CYP3A4, expressed in *E. coli*, was a gift from Josh Pearson, Department of Medicinal Chemistry, University of Washington.

Human liver microsomes, devoid of significant amounts of CYP3A5 protein, were selected from the University of Washington Human Liver Bank and equal amounts of microsomal protein from the five different preparations were pooled for subsequent experimentation (Isoherranen et al., 2004).

In vitro incubations. Stereoselective metabolism of ITZ was studied *in vitro* using heterologously expressed CYP3A4 (Supersomes). ITZ stereoisomers were dissolved in

acetonitrile and added to the incubations at a concentration of 10 or 50 μM to give a final acetonitrile concentration in all incubations of 1% and concentrations of the ITZ stereoisomers of 100 nM and 500 nM. The incubations were performed in 100 mM potassium phosphate (KPi) buffer (pH 7.4) with 1 mM EDTA using a concentration of 10 pmol/ml CYP3A4 (0.084 mg microsomal protein/ml). All incubations were performed in duplicate. A starting incubation volume of 1.8 ml was employed. After preincubation for 4 min at 37°C, the reaction was initiated with NADPH (final concentration 1 mM). At 0, 1, 2, 5, and 10 min, 200 μl samples were transferred to tubes containing 200 μl of ice-cold acetonitrile to quench the reaction. The samples were vortexed, centrifuged at 10000 g for 10 min, and the supernatant transferred to an HPLC vial for LC-MS analysis. The concentrations of the parent ITZ stereoisomers and the metabolites (OH-ITZ, keto-ITZ and ND-ITZ) were determined using a previously described LC-MS method (Isoherranen et al., 2004).

Inhibition of CYP3A4 by itraconazole stereoisomers. IC_{50} values for (2R,4S,2'R)-ITZ, (2R,4S,2'S)-ITZ, (2S,4R,2'R)-ITZ and (2S,4R,2'S)-ITZ inhibition of the CYP3A4 catalyzed 1′-hydroxylation of midazolam (MDZ) were determined. The incubations were carried out in duplicate in 100 mM KPi buffer (pH 7.4) with 1 mM EDTA and 5 pmol/ml CYP3A4. The NADPH concentration in all incubations was 1 mM. A sub K_m concentration of 1 μM midazolam was used in all incubations. ITZ stereoisomers were added to the 500 μl incubations at nominal concentrations of 0, 5, 25, 50, 100, 250, 500 and 1000 nM. After preincubation for 4 min at 37°C, the reaction was initiated with NADPH (final concentration 1 mM). At 0 min and 2 min, a 200 μl sample was collected into a vial containing 200 μl of ice-cold acetonitrile. Internal standard solution (D_2-labeled OH-MDZ, 100 ng/ml, 10 μl) was added and the mixture was vortexed and centrifuged. The inhibitor concentration was measured at time 0 min and at time 2

min and the mean inhibitor concentration was calculated for the incubation period (i.e. the inhibitor concentration was corrected for depletion). The concentration of OH-MDZ was measured in the 2 min sample.

Concentrations of OH-MDZ were measured using a Hewlett Packard series 1100 MSD system operating in the positive ion electrospray mode with selected ion monitoring using a previously reported method (Isoherranen et al., 2004). Separation was achieved using a Zorbax Eclipse XDB-C8 5 μm column (2.1 mm i.d. × 50 mm; Agilent Technologies) equipped with a Phenomenex SecurityGuard C8 guard column.

Determination of ligand induced binding spectra. The optical titrations of the ligand induced binding spectra were performed with an Aminco DW2 dual beam spectrophotometer as upgraded by Olis Instruments, Inc. Matched cuvettes containing CYP3A4 (370 nM) in KPi buffer (pH 7.4) with 20% glycerol (to stabilize the purified CYP3A4 and prevent denaturation and aggregation) at 37ºC were used. Ligand was added in 1 μl increments of 25 μM solution to the sample cuvette. Matching volumes of solvent (acetonitrile) were added into the reference cuvette. Ligand induced difference spectra were recorded using Supersomes and purified CYP3A4 with the mixture of itraconazole stereoisomers and identical (same extinction coefficient, and absorbance maximum and minimum) behavior of the two enzyme systems was confirmed. However, only purified CYP3A4 was used for the quantitative spectral titration experiments to improve spectral quality and decrease noise in the spectra. Use of purified CYP3A4 also allowed recording of absolute binding spectra of each ligand.

Clinical study design and blood sampling. Six healthy adult volunteers, two male and four female (age range 18-33 years), participated in the study after each had given written consent. The study protocol was approved by the institutional review board (IRB) of the University of

Washington and by the Scientific Advisory Committee of the General Clinical Research Center of the Medical Center of the University of Washington. The study consisted of a seven-day administration of ITZ oral solution (10 ml of 10 mg/ml once daily on the morning). The subjects fasted overnight prior to each ITZ dose. Blood samples (4 ml) were collected into heparinized collection tubes on day 1 and day 7 of the study at time points 0, 0.5, 1, 2, 3, 4, 6, 8, 12 and 24 h after drug administration via an indwelling venous catheter.

Determination of itraconazole and metabolite concentrations. Concentrations of ITZ, OH-ITZ, keto-ITZ and ND-ITZ in the inhibition experiments were measured by high performance liquid chromatography-mass spectrometry (LC-MS) using a Hewlett Packard series 1100 MSD system operating in the positive ion electrospray mode with selected ion monitoring and equipped with HP Chemstation data analysis software using a previously published method (Isoherranen et al., 2004). Analyte separation was achieved using a Zorbax Eclipse XDB-C8 5 μm column (2.1 mm i.d. × 50 mm; Agilent) equipped with a Phenomenex C8 guard column (2.1 mm i.d × 4 mm). Calibration curves for ITZ, OH-ITZ, keto-ITZ were prepared between concentrations 1 nM and 1000 nM. For ND-ITZ, the concentration range was 1 nM to 100 nM. The limits of detection for ITZ and its metabolites were 1 nM and the limits of quantification were at 5 nM.

Stereoselective analysis. A steroselective HPLC-MS assay was developed to analyze the concentrations of itraconazole stereoisomers in plasma and to determine the absolute configuration of formed metabolites. The stereoisomers were separated using a Chiralpak AS-RH 5 μm column (150 mm × 2.1 mm i.d., Chiral Technologies Inc. Exton, PA) with a mobile phase flow rate of 0.2 ml/min. The initial mobile phase was 30% acetonitrile 70% aqueous 5 mM ammonium acetate. The acetonitrile concentration increased linearly to 70% between 4 and 50

DMD Fast Forward. Published on January 13, 2006 as DOI: 10.1124/dmd.105.008508
This article has not been copyedited and formatted. The final version may differ from this version.

minutes, then to 80% over additional two minutes. Ions monitored were m/z 705 for ITZ, m/z 721 for OH-ITZ, m/z 719 for keto-ITZ and m/z 649 for ND-ITZ, all [MH^+]-ions. The drying gas flow was set at 10 L/min, nebulizer pressure at 25 psig, gas temperature at 300 ºC and the capillary voltage at 5500 V. The fragmentor was set at 160 V for all ions. The incubation samples were prepared identically to the non-chiral assay. For plasma samples, 300 µl of acetonitrile was added to 100 µl of plasma, and the samples were centrifuged at 10000 g for 10 minutes and then transferred to autosampler vials. A 20 µl sample was injected on column. Only two of the four stereoisomers of ITZ were clearly separated using this method; the (2R,4S,2'R)-ITZ and (2R,4S,2'S)-ITZ eluted together (Figure 3a). Therefore, pharmacokinetic analysis was conducted separately for the two pairs of stereoisomers based on their dioxolane ring stereochemistry, (2R,4S,2'R)-ITZ and (2R,4S,2'S)-ITZ as one pair and (2S,4R,2'R)-ITZ and (2S,4R,2'S)-ITZ as a second pair. The keto-ITZ stereoisomer eluted as three peaks and the elution order of the keto-ITZ stereoisomers was assumed to follow the elution order of the corresponding stereoisomers of ITZ (Figure 3a). This allowed tentative assignments of the peaks corresponding to (2R,4S)-keto-ITZs and (2S,4R)-keto-ITZs. Similarly, it was assumed that the ND-ITZ stereoisomers eluted in a similar order based on the stereochemistry on the dioxolane ring as the ITZ stereoisomers; i.e. the (2S,4R) stereoisomers eluting first. It was not possible to separate all eight of the OH-ITZ stereoisomers in the commercial mixture and of these, only the four (2R,4S)-stereoisomers were available. Therefore only partial characterization of the formation OH-ITZ stereoisomers was possible.

Data analysis. All non-linear fitting was performed using Winnonlin (Pharsight Corp) data analysis software. All pharmacokinetic parameters were obtained using the noncompartmental approach and standard pharmacokinetic methods. The peak concentrations (C_{max}) and times at

DMD Fast Forward. Published on January 13, 2006 as DOI: 10.1124/dmd.105.008508
This article has not been copyedited and formatted. The final version may differ from this version.

which peak concentrations were reached (t_{max}) were obtained directly from the plasma concentration *vs.* time data. IC_{50} values were calculated by standard non-linear fit to the data. The K_s values for ITZ stereoisomers were obtained by fitting the "Morrison" equation (Segel 1993) to the spectral titration data:

$$[ES] = \frac{([E]+[S]+K_S) - \sqrt{([E]+[S]+K_S)^2 - 4[E][S]}}{2}$$

in which [E] is the total CYP3A4 concentration in solution, [S] is the total substrate concentration added and [ES] is the concentration of the CYP3A4-ITZ complex as calculated from the titration data using the extinction coefficient for [ES] measured from the ratio of absorbance (difference of absorbance between 424nm and 390nm) at saturation and the total enzyme concentration.

Statistical analysis. Data are expressed as mean values $\pm$ SD (standard deviation). Statistical analysis was performed with the Systat statistical analysis program (SYSTAT Inc. Evanston, IL). The Wilcoxon matched pair test was used to compare the peak and trough concentrations between the two pairs of stereoisomers.

RESULTS

Stereoselective metabolism of itraconazole in vitro. Metabolism of ITZ was dependent on the stereochemistry of the dioxolane ring. Incubations of the individual ITZ stereoisomers with heterologously expressed CYP3A4 showed that OH-ITZ is formed only from the two (2R,4S)-ITZ-stereoisomers, (2R,4S,2'R)-ITZ and (2R,4S,2'S)-ITZ. No OH-ITZ formation could be detected for (2S,4R,2'S)-ITZ and (2S,4R,2'R)-ITZ, even at high substrate concentrations (1000 nM) and an incubation time of 30 min. The absence of (2S,4R,2'S)-ITZ and (2S,4R,2'R)-ITZ metabolism by CYP3A4 was further confirmed by showing that no significant depletion of these

stereoisomers occurred in the incubations. Results from experiments with pooled human liver microsomes confirmed the results obtained using the expressed enzyme system: OH-ITZ was formed only from the (2R,4S)-stereoisomers in human liver microsomes.

CYP3A4-catalyzed 3'-hydroxylation of the ITZ side-chain can produce as many as four possible OH-ITZ stereoisomers from the two (2R,4S)-ITZ stereoisomers: (2R,4S,2'S,3'R)-OH-ITZ, (2R,4S,2'R,3'S)-OH-ITZ, (2R,4S,2'S,3'S)-OH-ITZ and (2R,4S,2'R,3'R)-OH-ITZ. Separation of (2R,4S,2'S,3'S)-OH-ITZ from the three other (2R,4S)-OH-ITZ stereoisomers was attained (Figure 3d), but separation of all four of these stereoisomers of OH-ITZ was not achieved. Analysis of the hydroxylated products from incubations of (2R,4S,2'S)-ITZ showed that (2R,4S,2'S,3'R)-OH-ITZ was formed whereas only trace amounts of (2R,4S,2'S,3'S)-OH-ITZ were detected (Figure 3b), demonstrating stereoselective formation of the hydroxylated metabolite. Separation of the two possible OH-ITZ stereoisomers formed from (2R,4S,2'R)-ITZ was not achieved and therefore similar analysis could not be conducted for this stereoisomer. A greater amount of OH-ITZ was formed from (2R,4S,2'S)-ITZ. After a 10 minute incubation, the amount of OH-ITZ produced from (2R,4S,2'S)-ITZ was approximately 5 times that produced from (2R,4S,2'R)-ITZ (21 pmol versus 3.8 pmol in 200 μl, respectively).

Sequential metabolism was observed in incubations with both (2R,4S)-ITZ stereoisomers. Keto-ITZ and ND-ITZ, both of the (2R,4S)-configuration based on analogous retention pattern as with ITZ (Figure 3a and 3b), were detected in all incubations with these stereoisomers of ITZ. The formation of keto-ITZ and ND-ITZ from the four different OH-ITZ stereoisomers with the (2R,4S)-stereochemistry of the dioxolane ring was confirmed in incubations of the individual stereoisomers with heterologously expressed CYP3A4 (data not

shown). Based on the experiments described above, a scheme for the sequential metabolism of ITZ stereoisomers was constructed (Figure 4).

Inhibition and binding of CYP3A4 by itraconazole stereoisomers. The inhibition of CYP3A4 mediated midazolam hydroxylation by the stereoisomers of ITZ was studied using CYP3A4 Supersomes. Despite the short incubation time (2 min), significant depletion of (2R,4S,2'S)-ITZ and (2R,4S,2'R)-ITZ was observed in incubations with the nominal inhibitor concentrations below 100 nM. Formation of OH-ITZ and keto-ITZ was observed in all of these incubations as well. Concentrations of metabolites produced in these incubations were 2-44 nM for OH-ITZ and 1-12 nM for keto-ITZ. In some incubations with the (2R,4S)-ITZ isomers, the concentration of OH-ITZ exceeded that of ITZ. Neither depletion of the inhibitor nor formation of any metabolites was observed in incubations using either (2S,4R,2'S)-ITZ or (2S,4R,2'R)-ITZ as the inhibitor. Their apparent IC_{50} values are summarized in Table 1, and a determination of a representative IC_{50} value is shown in Figure 5. Interestingly, the two ITZ stereoisomers that underwent metabolism by CYP3A4 also had two- to four-fold lower IC_{50} values than the stereoisomers that were not metabolized. It was not possible to separate the inhibitory contribution of the metabolites from the contribution of the parent drug isomers and it should be noted that the lower IC_{50} values might be a result of inability to account for the effects of additional inhibitory species. Therefore, in order to compare the intrinsic binding affinity of the ITZ stereoisomers to CYP3A4, spectral titrations with the stereoisomers were undertaken and their K_s values were determined.

All four ITZ stereoisomers, regardless of their ability to undergo metabolism by CYP3A4, induced type II binding spectra with purified CYP3A4, suggesting that the triazole nitrogen of these compounds coordinates the heme iron of CYP3A4. The spectral characteristics

obtained from the stereoisomers that were metabolized were indistinguishable from the stereoisomers that were not metabolized by CYP3A4; the difference spectrum of each compound was characterized by a maximum at 434 nm and minimum at 390 nm. From these spectral titrations, it appeared that (2R,4S)-ITZ pair might have a slightly higher apparent extinction coefficient with CYP3A4 than the (2S,4R)-ITZ pair, but the difference was not significant. All four stereoisomers exhibited high affinity for CYP3A4. The K_s-values for the four ITZ stereoisomers are summarized in Table 1. Due to the depletion of free ligand by binding to CYP3A4, the quadratic equation (Morrison equation) was fitted to the spectral titration data. The spectral titration and the fit of the Morrison equation to the data from (2S,4R,2'S)-ITZ is shown in Figure 5.

Stereoselective pharmacokinetics of itraconazole in vivo. The disposition of ITZ was studied in 6 healthy subjects following single and multiple doses of ITZ. Since incomplete chromatographic separation of (2R,4S,2'R)-ITZ and (2R,4S,2'S)-ITZ was obtained, the pharmacokinetic parameter estimates for this pair of stereoisomers were calculated as the sum of the total concentration of (2R,4S,2'R)-ITZ and (2R,4S,2'S)-ITZ. For comparison, the plasma concentrations of (2S,4R,2'R)-ITZ and (2S,4R,2'S)-ITZ were added and pharmacokinetic analysis was performed on the sum of these two stereoisomers. The plasma concentration versus time curves of the (2S,4R,2'R)-ITZ and (2S,4R,2'S)-ITZ were superimposable and these two stereoisomers had identical pharmacokinetic characteristics (data not shown). The analysis of the two pairs instead of each stereoisomer separately was justified based on the stereoselective metabolism of the stereoisomers by CYP3A4 in vitro. The pharmacokinetic analysis was essentially performed for the stereoisomers that undergo metabolism by CYP3A4 in vitro versus those that do not.

Full stereoselective pharmacokinetic analysis was carried out in one of the six subjects (subject E). The plasma concentration versus time curves of the ITZ stereoisomeric pairs on study day 1 and day 7 in this subject are shown in Figure 6. The pharmacokinetic parameter estimates obtained are presented in Table 2. The disposition of ITZ was stereoselective in this subject and the stereoselective indexes (the parameter ratio between the high and low stereoisomer pair value) ranged from 2.0 to 7.2. The largest difference between the stereoisomeric pairs was observed in oral clearance. On day 1, the (2R,4S)-ITZ pair had over 7 fold greater oral clearance than the (2S,4R)-ITZ pair. The apparent terminal half-life of the (2R,4S)-ITZ pair was half of that of the (2S,4R)-ITZ pair. The pharmacokinetic parameters obtained on day 1 differed from those of day 7 for both stereoisomeric pairs in this subject. For the (2R,4S)-ITZ pair the AUC increased 6.9 fold (AUC_{inf} vs AUC_{0-24}) with a corresponding decrease in oral clearance. The C_{max} of the (2R,4S)-ITZ pair increased 5.5-fold between the two study occasions. For the (2S,4R)-ITZ pair the increase in AUC and C_{max} was more modest, 2-fold, between day 1 and day 7 of the study. Stereoselective pharmacokinetics was observed on day 7 of the study, at steady state, but to a lesser extent than on day 1. At steady state, the AUC of the (2S,4R)-ITZ pair was three times the AUC for the (2R,4S)-ITZ pair. Interestingly, in this subject the difference in the C_{max} value between the two pairs of stereoisomers disappeared at steady state suggesting loss of a stereoselective first pass effect.

The peak and trough concentrations were analyzed for all six volunteers and the results are shown in Table 3. On day one of the study, the peak concentration of the (2S,4R)-ITZ pair was 3 times, and the trough concentrations were 10 times those of the (2R,4S)-ITZ pair ($p<0.05$). The difference decreased at steady state, and on day 7 of the study, the peak concentration of the (2S,4R)-ITZ pair was only 1.5-fold greater, and the trough concentrations 4-fold greater than the

(2R,4S)-ITZ pair but the difference was still significant ($p<0.05$). Accumulation, demonstrated by a significant increase in the trough concentrations between day 1 and day 7 of the study, was observed for both stereoisomeric pairs, although it was greater for the (2R,4S)-pair; 20-fold for (2R,4S)-ITZ and 8-fold for (2S,4R)-ITZ.

The peak and trough plasma samples of the volunteers as well as the plasma samples of subject E were analyzed for stereochemistry of OH-ITZ, keto-ITZ and ND-ITZ metabolites. In plasma, ND-ITZ and keto-ITZ were of the (2R,4S)-configuration (Figure 3c). Because OH-ITZ potentially consists of 8 stereoisomers, the absolute configuration of the formed OH-ITZ could not be confirmed, but the lack of formation of (2R,4S,2'S,3'S)-OH-ITZ in vivo was established since this stereoisomer was separated chromatographically from the others.

To estimate the relative contribution of the individual pairs of itraconazole stereoisomers to the in vivo inhibition of CYP3A4, the ratios between the peak and trough plasma concentrations and the IC_{50} values were calculated (Table 4). All values except the trough concentration/IC_{50} on day 1 for (2R,4S)-ITZ were greater than 1 suggesting that both stereoisomer pairs would cause an in vivo drug-drug interaction but the relative contribution of the different stereoisomers varied over the dosing interval as suggested by the change in the ratio between parameter values for the stereoisomer pairs.

DISCUSSION

The goals of this study were to determine whether the binding of ITZ to CYP3A4, the metabolism of ITZ by CYP3A4 and the pharmacokinetic behavior of ITZ in vivo are stereoselective. The major finding is that the metabolism of ITZ by CYP3A4 is highly stereoselective. Only two of the four ITZ stereoisomers underwent metabolism by CYP3A4.

The major stereochemical determinant in the metabolism of ITZ is the absolute stereochemistry of the dioxolane ring portion of the molecule. It was notable that the dioxolane ring remote from the site of metabolism had such a critical effect on oxidation of ITZ. One possibility is that some active site residue(s) steers the molecule into the metabolically productive orientation; perhaps via coordination of the triazole to an acidic amino acid at the active site. Further experiments are needed to more thoroughly assess the influence of the dioxolane ring on the orientation of ITZ stereoisomers at the CYP3A4 active site.

Stereochemistry of the 2' position of ITZ pyrazolone-butyl side chain also affected oxidation. For (2R,4S,2'S)-ITZ, 5 times the amount of OH-ITZ was produced when compared to (2R,4S,2'R)-ITZ under these experimental conditions. Based on the similar IC_{50} and K_s values, the affinity of both stereoisomers for CYP3A4 was similar and therefore the larger amount of OH-ITZ formed from (2R,4S,2'S)-ITZ suggests a faster catalytic rate from this stereoisomer. The K_m and V_{max} of (2R,4S,2'S)-ITZ and (2R,4S,2'R)-ITZ were not determined because the metabolism of itraconaole stereoisomers is complicated by sequential metabolism, formation of inhibitory metabolites and potential multiple binding orientations in the active site. Future experiments will be needed to characterize and model the kinetics of the sequential oxidations of these stereoisomers.

The mixture of ITZ stereoisomers induces a characteristic type II binding spectrum with CYP3A4, suggesting that a triazole-ring nitrogen coordinates with the heme iron, producing a characteristic low spin complex. However, ITZ also undergoes metabolism by CYP3A4 at the aliphatic side chain distal to the triazole nitrogens. The apparent existence of at least two distinct enzyme-substrate complexes leads to the hypothesis that the two stereoisomers of ITZ that undergo metabolism by CYP3A4 would yield a type I binding spectrum with CYP3A4 and the two that are not turned over would demonstrate type II binding spectra. However, it was not possible to differentiate spectrally between the binding of the two stereoisomers that undergo metabolism and the two that do not, since all four ITZ stereoisomers produced a type II binding spectrum of similar intensity. This observation demonstrates that the triazole nitrogen accesses and coordinates the heme iron, regardless of the absolute stereochemistry in the dioxolane ring of ITZ, but stereochemistry is a crucial determinant for a second, metabolically productive orientation. At present, it is not known whether the two stereoisomers of ITZ that are not turned over by CYP3A4 have two different orientations at the active site of CYP3A4. It is likely, however, that the inhibition of CYP3A4 by these two stereoisomers, (2S,4R), is due to the coordination of CYP3A4 heme by the triazole nitrogen.

The stereoselective disposition of ITZ in vivo reflects the stereoselective metabolism of ITZ by CYP3A4 and supports the conclusion that CYP3A4 is important for elimination of ITZ. The stereoisomer pair that is metabolized by CYP3A4 ((2R,4S,2’R)-ITZ and (2R,4S,2’S)-ITZ), had higher oral clearance and smaller AUC than the other pair (2S,4R,2’S)-ITZ and (2S,4R,2’R)-ITZ, in vivo. The seven-fold difference in oral clearance between the stereoisomeric pairs on day 1 is most likely due to stereoselectivity in the first pass metabolism, as well as hepatic metabolic clearance of ITZ. The contribution of gut metabolism to the stereoselective pharmacokinetics of

ITZ is also supported by the more modest stereoselectivity in the half-life when compared to oral clearance and AUC.

Presumably, as a consequence of the stereoselective metabolism of the (2R,4S)-ITZs during first pass, the peak concentrations of this pair were significantly lower than those of the (2S,4R)-pair. Interestingly, stereoselectivity was diminished at day 7 of the pharmacokinetic study. The decrease in stereoselectivity might be attributed to auto-inhibition of intestinal and possibly hepatic CYP3A4 by the ITZ stereoisomers, leading to reduced first pass metabolism. Auto-inhibition of CYP3A4 is also in agreement with the greater than predicted accumulation of (2R,4S)-ITZ. It is noteworthy, that despite the shorter half-life after single dose, based on the increased trough levels the (2R,4S)-ITZ stereoisomers accumulated significantly more than the (2S,4R)-ITZ stereoisomers. This observation supports the view that the auto-inhibition observed after multiple doses of the four ITZ stereoisomers is due to saturation of CYP3A4 mediated metabolism of (2R,4S)-ITZ pair. Also, based on the in vitro stereoselective metabolism data (including substrate depletion experiments), a maximum of 50% of the systemic clearance of ITZ is CYP3A4 mediated.

Interpretation of the pharmacokinetic data of ITZ stereoisomers is complicated by possible stereoisomer-stereoisomer interactions. All four ITZ stereoisomers are high affinity ligands of CYP3A4, and it is likely that the (2S,4R)-ITZ stereoisomers inhibit the elimination of the (2R,4S)-ITZ's at steady state. The higher plasma concentrations of (2S,4R)-ITZ at steady state and after single dose suggest that a significant portion of the hepatic CYP3A4 is bound by these stereoisomers, despite the fact that they are not substrates of CYP3A4. It is also possible that the kinetic non-linearity after ITZ dosing is a result of stereoisomer-stereoisomer interaction instead of saturation of the enzyme by the species undergoing metabolism. In order to obtain

additional information about the mechanisms of kinetic non-linearity, each of the ITZ stereoisomers should be administered separately to humans.

In previous studies, where stereochemical factors were not explored, the half-life of OH-ITZ has been found to be consistently shorter than that of the parent compound and it has been suggested that this phenomenon reflects predominant formation of OH-ITZ during the first pass (Ducharme et al., 1995). In this study it was hypothesized that the half-life of OH-ITZ is dependent on the half-life of the stereoisomers of ITZ that undergo metabolism by CYP3A4 and therefore contribute to the formation of OH-ITZ in vivo following classical formation rate limited kinetics. Indeed, the half-life of (2R,4S)-ITZs, 10 hours, was shorter than or equal to that calculated for OH-ITZ in this subject (10-14 hours), in agreement with formation rate limited metabolite kinetics. However, the plasma concentration versus time curves of ITZ stereoisomers still showed biphasic elimination, despite the stereoselective analysis, consistent with significant tissue distribution.

A modest stereoselective ratio was observed in the IC_{50}-values for ITZ stereoisomers, although it is not clear whether this is due to contribution of the formed inhibitory metabolites. A previous study has shown that the inhibition of CYP3A4 by ketoconazole, a related azole antifungal, is stereoselective (Dilmaghanian et al., 2004). Whether the metabolism of ketoconazole by CYP3A4 is stereoselective as well has not been reported. It is not immediately evident which stereoisomers of ITZ are most important in terms of in vivo inhibition of CYP3A4 and drug-drug interactions. On day 1 the ratio between C_{max} and IC_{50} was 23.4 for both stereosiomer pairs (Table 4) but at the trough concentration, a five-fold greater ratio of C_{min}/IC_{50} was observed for the (2S,4R)-ITZ-pair. In contrast, on day 7 (steady state) of the study, the C_{max} to IC_{50} ratio was twice as high for the (2R,4S)-ITZ pair as for the (2S,4R)-ITZ pair and C_{min}/IC_{50}

value was approximately equal for the two pairs. At present, it is not possible to conclude which stereoisomer contributes the most to clinical inhibition of CYP3A4. In addition, it is likely that the circulating metabolites do contribute to CYP3A4 inhibition, but the inhibitory potency of the stereoisomers of the metabolites has not yet been determined.

The results presented here suggest that a single ITZ stereoisomer, i.e. (2S,4R,2'R)-ITZ or (2S,4R,2'S)-ITZ) might be clinically superior to the mixture of ITZ stereoisomers. This would have advantages over the currently used stereoisomer mixture. It would not undergo metabolism by CYP3A4, eliminating the formation of inhibitory metabolites and having potentially more predictable multiple dose kinetics than the mixture of stereoisomers, its elimination would not be subject to stereoisomer-stereoisomer interactions *via* CYP3A4, it would have equivalent plasma concentrations after administration of lower doses of drug due to lower oral clearance, and it may be a less potent inhibitor of CYP3A4 than the other stereoiosmers based on its IC_{50} and lack of inhibitory metabolites. In addition, based on the patent data (Koch et al., 2000), this stereoisomer should be a more potent antifungal than the mixture.

In conclusion, this study showed that the pharmacokinetic behavior of ITZ is stereoselective, most likely due to stereoselective metabolism of ITZ by CYP3A4. All stereoisomers bind to the CYP3A4 heme by the triazole nitrogen, but at least two of the stereoisomers (the (2R,4S)-pair) also adopt to a binding orientation in which the alkyl- side chain is presented to the heme iron. Thus, predicting in vivo inhibition of CYP3A4 by the itraconazole stereoisomer mixture currently administered is exceedingly complicated, due to different plasma concentrations and inhibitory potencies of the stereoisomers, formation of inhibitory metabolites, and potential enatiomer-enantiomer interactions between the stereoisomers.

REFERENCES

Backman JT, Kivisto KT, Olkkola KT and Neuvonen PJ (1998) The area under the plasma concentration-time curve for oral midazolam is 400-fold larger during treatment with itraconazole than with rifampicin. *Eur J Clin Pharmacol* **54:**53-58.

Barone JA, Koh JG, Bierman RH, Colaizzi JL, Swanson KA, Gaffar MC, Moskovitz BL, Mechlinski W and Van de Velde V (1993) Food interaction and steady-state pharmacokinetics of itraconazole capsules in healthy male volunteers. *Antimicrob Agents Chemother* **37:**778-784.

Breadmore MC and Thormann W (2003) Capillary electrophoresis evidence for the stereoselective metabolism of itraconazole in man. *Electrophoresis* **24:**2588-2597.

Dilmaghanian S, Gerber JG, Filler SG, Sanchez A and Gal J (2004) Enantioselectivity of inhibition of cytochrome P450 3A4 (CYP3A4) by ketoconazole: Testosterone and methadone as substrates. *Chirality* **16**:79-85.

Ducharme MP, Slaughter RL, Warbasse LH, Chandrasekar PH, Van de Velde V, Mannens G and Edwards DJ (1995) Itraconazole and hydroxyitraconazole serum concentrations are reduced more than tenfold by phenytoin. *Clin Pharmacol Ther* **58:**617-624.

Florea NR, Capitano B, Nightingale CH, Hull D, Leitz GJ and Nicolau DP (2003) Beneficial pharmacokinetic interaction between cyclosporine and itraconazole in renal transplant recipients. *Transplant Proc* **35:**2873-2877.

Haria M, Bryson HM and Goa KL (1996) Itraconazole. A reappraisal of its pharmacological properties and therapeutic use in the management of superficial fungal infections. *Drugs* **51:**585-620.

Heeres J, Backx LJ and Van Cutsem J (1984) Antimycotic azoles. 7. Synthesis and antifungal properties of a series of novel triazol-3-ones. J Med Chem **27**:894-900.

Heykants J, Van Peer A, Van de Velde V, Van Rooy P, Meuldermans W, Lavrijsen K, Woestenborghs R, Van Cutsem J and Cauwenbergh G (1989) The clinical pharmacokinetics of itraconazole: an overview. *Mycoses* **32 Suppl 1:**67-87.

Hutt AJ and Tan SC (1996) Drug chirality and its clinical significance *Drugs.* **52 Suppl 5**:1-12.

Isoherranen N, Kunze KL, Allen KE, Nelson WL and Thummel KE (2004) Role of itraconazole metabolites in CYP3A4 inhibition *Drug Metab Dispos.* **32:**1121-1131.

Koch P, Rossi RF Jr., Senanayake CH and Wald SA, inventors, (2000) Sepracor, Inc., assignee, 2R,4S-Hydroxyitraconazole Isomers, US Patent 6,147,077 (2000).

Levy RH and Boddy AV (1991) Stereoselectivity in pharmacokinetics: a general theory. *Pharm Res*. **8**:551-556

Mahnke CB, Sutton RM, Venkataramanan R, Michaels M, Kurland G, Boyle GJ, Law YM, Miller SA, Pigula FA, Gandhi S and Webber SA (2003) Tacrolimus dosage requirements after initiation of azole antifungal therapy in pediatric thoracic organ transplantation. *Pediatr Transplant* **7:**474-478.

Neuvonen PJ, Kantola T and Kivisto KT (1998) Simvastatin but not pravastatin is very susceptible to interaction with the CYP3A4 inhibitor itraconazole. *Clin Pharmacol Ther* **63:**332-341.

Olkkola KT, Ahonen J and Neuvonen PJ (1996) The effect of systemic antimycotics, itraconazole and fluconazole, on the pharmacokinetics and pharmacodynamics of intravenous and oral midazolam. *Anesthesia and Analgesia* **82:**511-516.

Poirier JM and Cheymol G (1998) Optimisation of itraconazole therapy using target drug concentrations. *Clin Pharmacokinet* **35:**461-473.

Segel IH. Enzyme Kinetics. Behavior and analysis of rapid equilibrium and steady-state systems. Wiley 1993 pp.

Tucker GT and Lennard MS (1990) Enantiomer specific pharmacokinetics. *Pharmac Ther* **45**:309-329.

Wedlund PJ, Aslanian WS, Jacqz E, McAllister CB, Branch RA, Wilkinson GR (1985) Phenotypic differences in mephenytoin pharmacokinetics in normal subjects. *J Pharmacol Exp Ther*. **234**:662-669.

Yamano K, Yamamoto K, Kotaki H, Sawada Y and Iga T (1999) Quantitative prediction of metabolic inhibition of midazolamby itraconazole and ketoconazole in rats: Implication of concentrative uptake of inhibitors into liver. *Drug Metab Dispos* **27:**395-402.

Yamano K, Yamamoto K, Katashima M, Kotaki H, Takedomi S, Matsuo H, Ohtani H, Sawada Y and Iga T (2001) Prediction of midazolam-CYP3A inhibitors interaction in the human liver from in vivo/in vitro absorption, distribution, and metabolism data. *Drug Metab Dispos* **29:**443-452.

FOOTNOTES

This study was supported in part by NIH PO1 GM32165, K24 DA00417 and P30 ES07033. A portion of this work was conducted through the Clinical Research Center Facility at the University of Washington and supported by the National Institutes of Health Grant M01-RR-00037.

FIGURE LEGENDS

Figure 1. Structures of the four stereoisomers of itraconazole (ITZ).

Figure 2. Structures of the metabolites of itraconazole: hydroxy-ITZ (OH-ITZ), keto-ITZ and N-desalkyl-ITZ (ND-ITZ). Only one of the possible stereoisomers formed in vivo is depicted for each metabolite.

Figure 3. Ion chromatograms demonstrating the stereoselective separation of itraconazole and its metabolites. a) Separation of reference mixtures of ITZ (4 stereoisomers), OH-ITZ (8 stereoisomers), keto-ITZ (4 stereoisomers) and ND-ITZ (2 stereoisomers). The peak annotation is as follows: A-(2R,4S)-ND-ITZ, B-(2S,4R)-ND-ITZ, C-(2R,4S)-keto-ITZ stereoisomer pair, D-(2S,4R,2'S)-keto-ITZ, E-(2S,4R,2'R)-keto-ITZ, F,G and H- unknown combinations of OH-ITZ stereoisomers, peak H has only (2S,4R)-stereochemistry, I-(2R,4S)-ITZ, J-(2S,4R,2'S)-ITZ, K-(2S,4R,2'R)-ITZ. The elution order of ITZ stereoisomers was determined to be (2R,4S,2'S)-ITZ, (2R,4S,2'R)-ITZ, (2S,4R,2'S)-ITZ and (2S,4R,2'R)-ITZ after injections of individual stereoisomers. For the OH-ITZ stereoisomers, (2R,4S,2'S,3'R)-OH-ITZ, (2R,4S,2'R,3'R)-OH-ITZ and (2R,4S,2'R,3'S)-OH-ITZ had identical retention times when injected separately. Only the four OH-ITZ stereoisomers with the (2R,4S) configuration were available and therefore it was not possible to identify the combination of stereoisomers eluting in each of the F, G and H peaks. The assignment of the elution order of the keto-ITZ stereoisomers ((2R,4S,2'S)-keto-ITZ and (2R,4S,2'R)-keto-ITZ first together, then (2S,4R,2'S)-keto-ITZ and (2S,4R,2'R)- keto-ITZ) and ND-ITZ stereoisomers was based on the elution order of the ITZ stereoisomers. b) Separation of the stereoisomers of ITZ metabolites in an incubation with (2R,4S,2'S)-ITZ. Peaks A and C are as described for panel a. Peak L was assigned as (2R,4S,2'S,3'R)-OH-ITZ based on comparison to reference material shown in panel d. c) stereoselective separation of ITZ and its

metabolites in the plasma of volunteer E. Peaks were assigned as described in panel a. d) Stereoselective separation of (2R,4S,2'S,3'S)-OH-ITZ (peak M) and (2R,4S,2'S,3'R)-OH-ITZ (peak L).

Figure 4. Scheme showing the stereoselective sequential metabolism pathways of itraconazole. The formation of both (2R,4S,2'R,3'R)-OH-ITZ and (2R,4S,2'R,3'S)-OH-ITZ from (2R,4S,2'R)-ITZ and the formation of ND-ITZ from both (2R,4S)-keto-ITZ stereoisomers has not been confirmed experimentally.

Figure 5. (a) Spectral titration of (2S,4R,2'S)-ITZ with CYP3A4. The lines represent the substrate induced binding spectra at increasing ITZ concentrations (50 nM-700 nM). (b) Determination of the binding constant for (2S,4R,2'S)-ITZ. The line represents the fit of the Morrison equation to the spectral titration data. (c) Inhibition of midazolam hydroxylation by (2S,4R,2'S)-ITZ. The line represents the best fit to determine the IC_{50}.

Figure 6. Plasma concentration versus time curves for the pairs of ITZ stereoisomers in subject E (a) on day 1 and (b) day 7 of the study.

TABLES

Table 1.

Binding characteristics of the four stereoisomers of ITZ.

	(2R,4S,2'R)-ITZ	(2R,4S,2'S)-ITZ	(2S,4R,2'R)-ITZ	(2S,4R,2'S)-ITZ
IC_{50} (nM)	4.0 ± 1.1	3.7 ± 4.1	14.8 ± 7.2	8.3 ± 4.2
K_s (nM)	2.2 ± 2.0	3.1 ± 1.7	10.6 ± 4.2	4.2 ± 1.2

DMD Fast Forward. Published on January 13, 2006 as DOI: 10.1124/dmd.105.008508
This article has not been copyedited and formatted. The final version may differ from this version.

Table 2.

Pharmacokinetic parameters for ITZ stereoisomer pairs in subject E following a single dose administration (day 1) of 100 mg oral solution of itraconazole and following multiple dose administration (100 mg/day) for 7 days.

Parameter	Day-1		Day-7	
	(2R,4S)-ITZ	(2S,4R)-ITZ	(2R,4S)-ITZ	(2S,4R)-ITZ
CL/F (L/h)	209	29	34	13
AUC[1] (h*nmol/L)	339	2460	2090	5640
$t_{1/2}$ (h)	9.0	19	10	25
C_{max} (nmol/L)	99	302	538	579

[1]For day 1 $AUC_{0\text{-}inf}$ and for day 7 $AUC_{0\text{-}24}$.

DMD Fast Forward. Published on January 13, 2006 as DOI: 10.1124/dmd.105.008508
This article has not been copyedited and formatted. The final version may differ from this version.

Table 3.

The peak and trough concentrations of the two enantiomeric pairs of ITZ in the six healthy volunteers after single dose administration (day 1) of 100 mg oral solution of itraconazole and following multiple dose administration (100 mg/day) for 7 days.

	Peak (day 1) (nM)	Trough (day 1) (nM)	Trough (day 6) (nM)	Peak (day 7) (nM)	Trough (day 7) (nM)
2R,4S-ITZs	91 ± 53	2.5 ± 2.6	43 ± 43	505 ± 74	47 ± 45
2S,4R-ITZs	270 ± 161	24 ± 14	172 ± 94	738 ± 84	182 ± 96
SI	3.0*	9.4*	4.0*	1.5*	3.8*

*Significant ($p<0.05$) difference found between the stereoisomer pairs

SI-stereoselectivity index- the parameter ratio between the high and low stereoisomer value presented to demonstrate the fold difference between the stereoisomer pairs.

DMD Fast Forward. Published on January 13, 2006 as DOI: 10.1124/dmd.105.008508
This article has not been copyedited and formatted. The final version may differ from this version.

Table 4.

The inhibitor concentration to IC_{50} ratios for the two pairs of ITZ stereoisomers calculated using peak and trough concentrations of the two enantiomeric pairs after single dose administration (day 1) of 100 mg oral solution of itraconazole and following multiple dose administration (100 mg/day) for 7 days.

	Day 1		Day 7	
	C_{max}/IC_{50}	C_{min}/IC_{50}	C_{max}/IC_{50}	C_{min}/IC_{50}
2R,4S-ITZ	23.4	0.6	130	12.1
2S,4R-ITZ	23.4	2.0	63.9	15.7

Fig 1

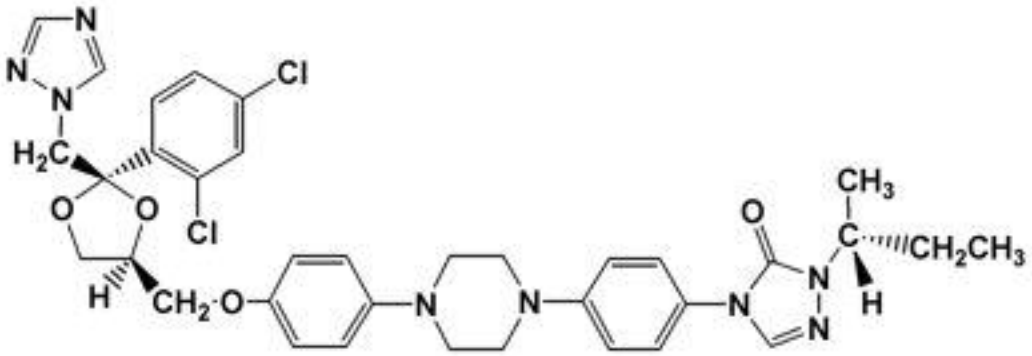

(2S,4R,2'R)-ITZ

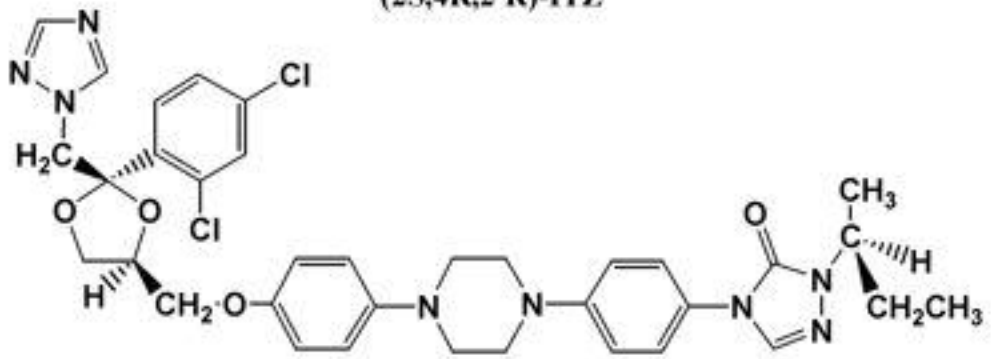

(2S,4R,2'S)-ITZ

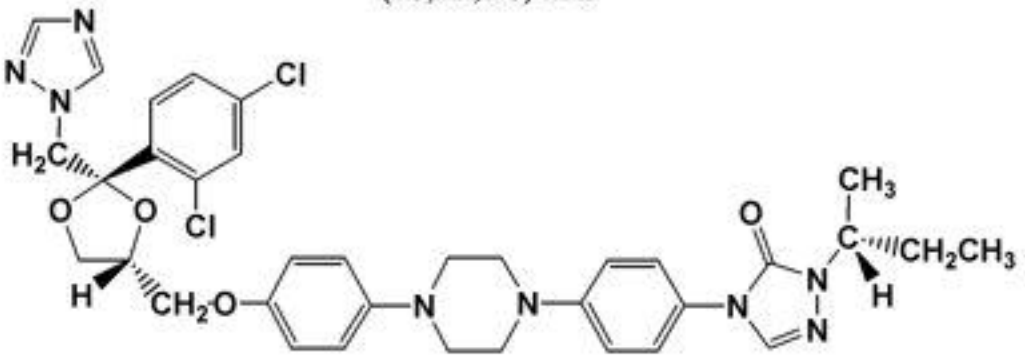

(2R,4S,2'R)-ITZ

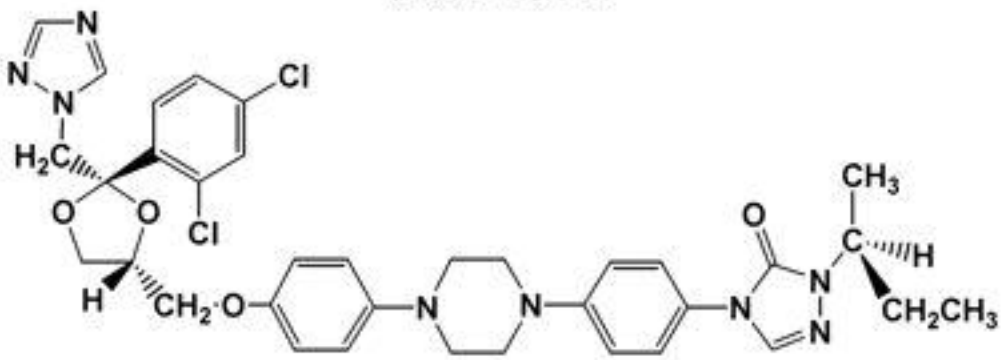

(2R,4S,2'S)-ITZ

Fig 2

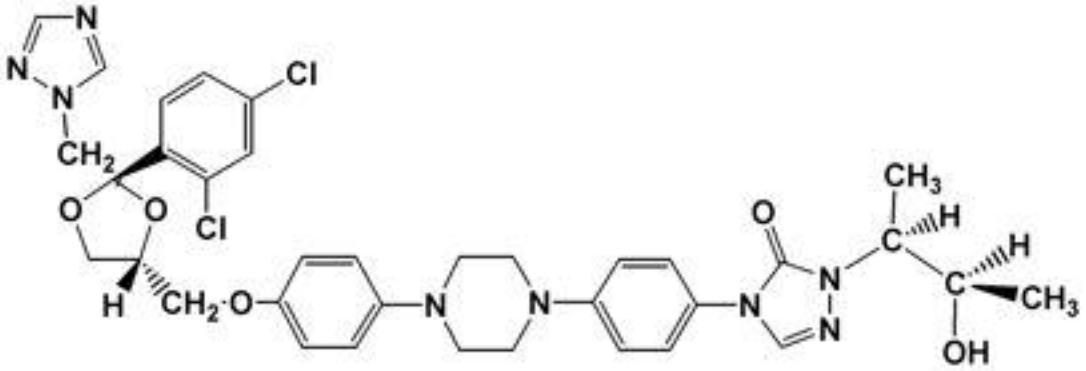

(2R,4S,2'S,3'R)-OH-ITZ

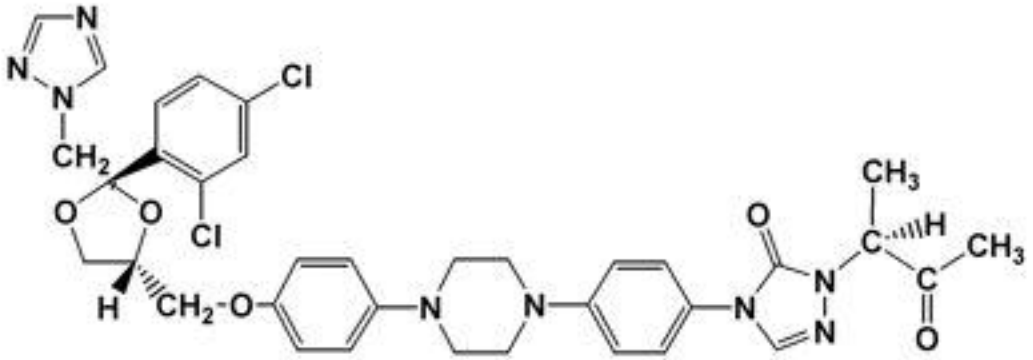

(2R,4S,2'S)-keto-ITZ

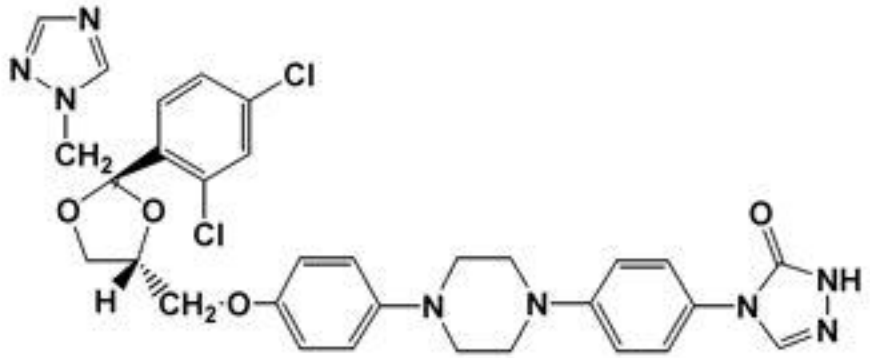

(2R,4S)-ND-ITZ

Fig3

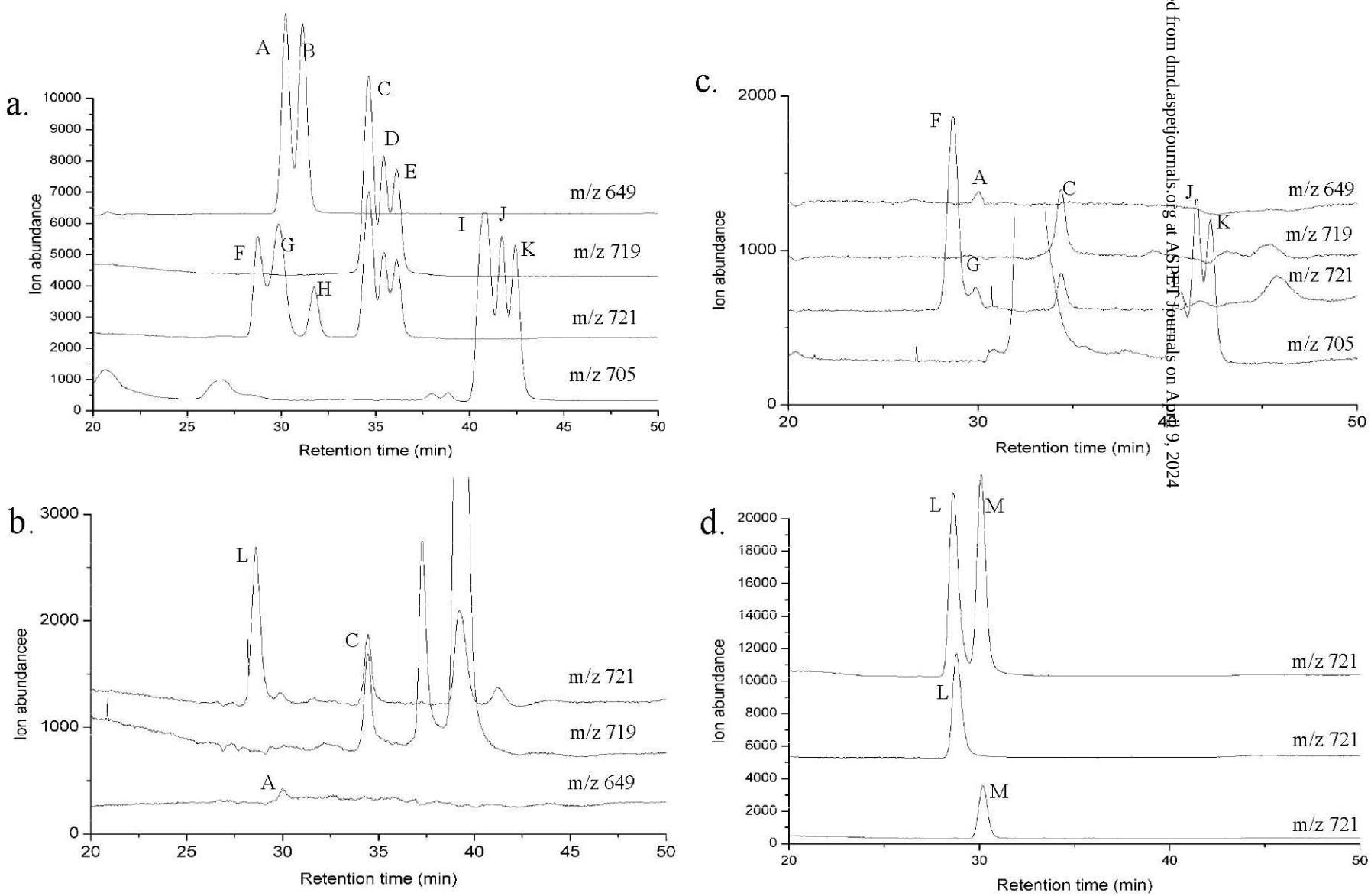

Fig 4

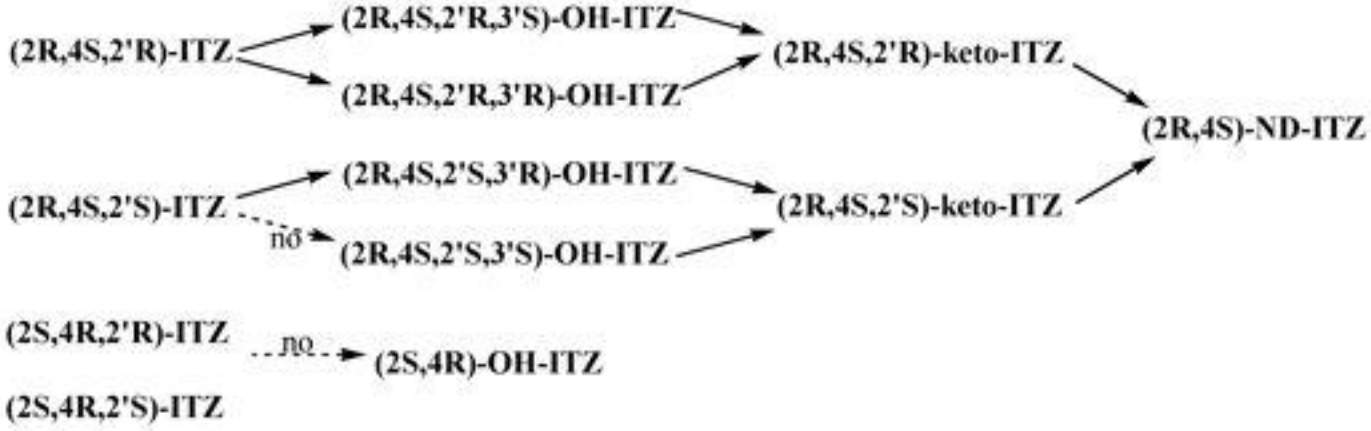
(2R,4S,2'R)-ITZ
(2R,4S,2'R,3'S)-OH-ITZ
(2R,4S,2'R,3'R)-OH-ITZ
(2R,4S,2'R)-keto-ITZ
(2R,4S)-ND-ITZ
(2R,4S,2'S)-ITZ
(2R,4S,2'S,3'R)-OH-ITZ
(2R,4S,2'S,3'S)-OH-ITZ
(2R,4S,2'S)-keto-ITZ
(2S,4R,2'R)-ITZ
(2S,4R,2'S)-ITZ
(2S,4R)-OH-ITZ

Fig 5

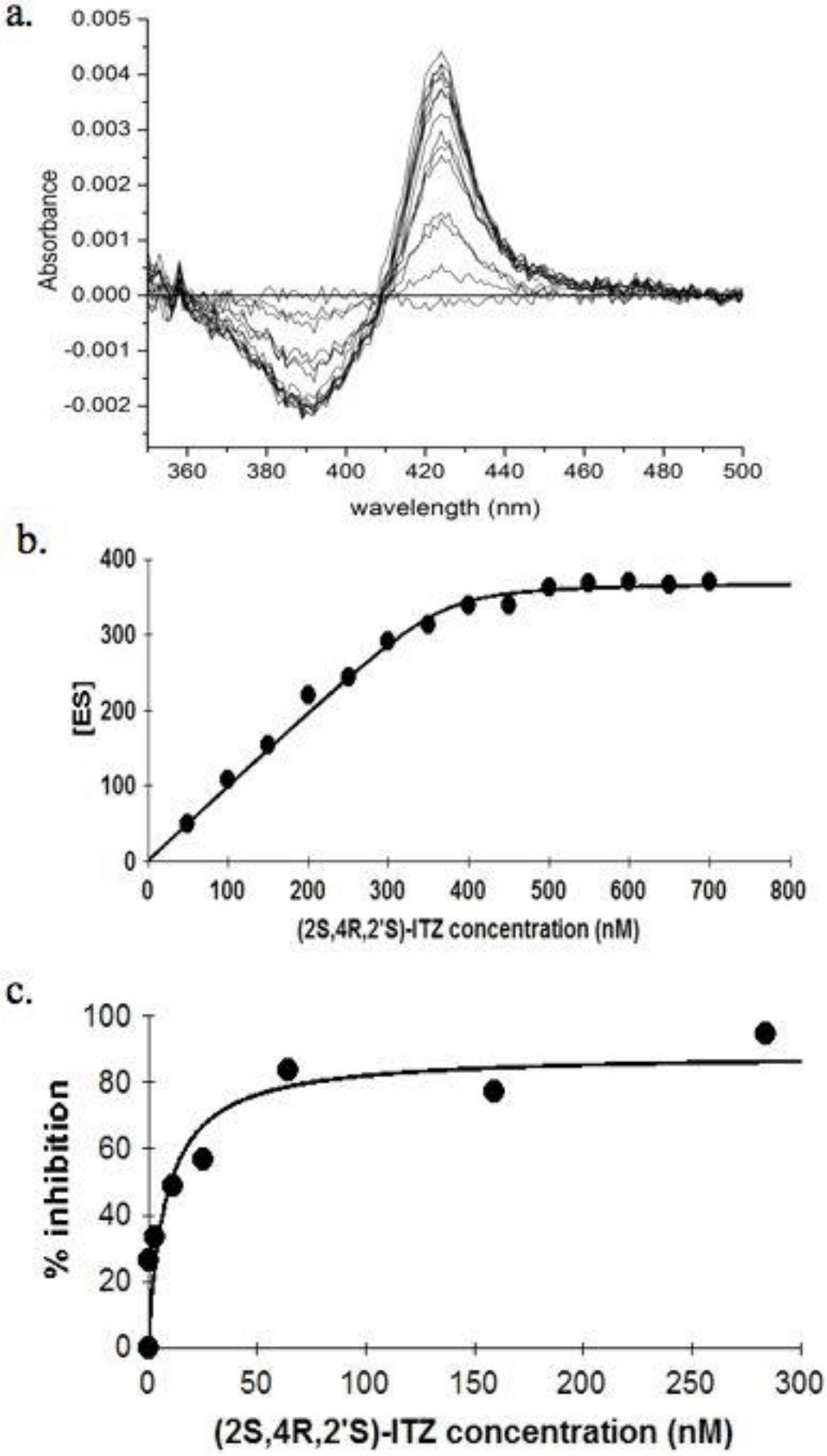
a.
Absorbance
0.005
0.004
0.003
0.002
0.001
0.000
-0.001
-0.002
360
380
400
420
440
460
480
500
wavelength (nm)
b.
[ES]
400
300
200
100
0
0
100
200
300
400
500
600
700
800
(2S,4R,2'S)-ITZ concentration (nM)
c.
% inhibition
100
80
60
40
20
0
0
50
100
150
200
250
300
(2S,4R,2'S)-ITZ concentration (nM)

Fig 6

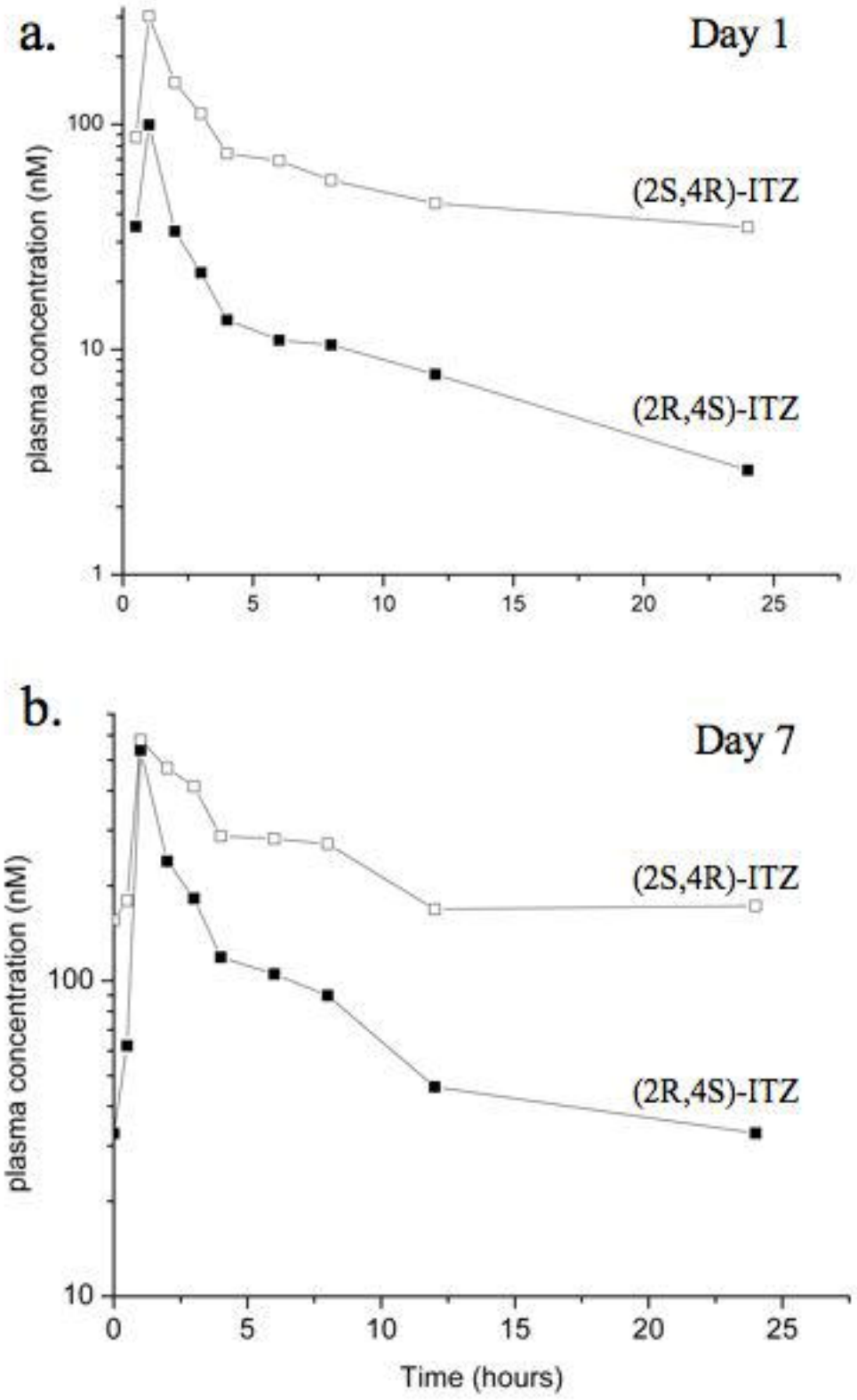
a.
Day 1
plasma concentration (nM)
100
10
1
0
5
10
15
20
25
(2S,4R)-ITZ
(2R,4S)-ITZ
b.
Day 7
plasma concentration (nM)
100
10
0
5
10
15
20
25
Time (hours)
(2S,4R)-ITZ
(2R,4S)-ITZ

Correction to "Stereochemical Aspects of Itraconazole Metabolism In Vitro and In Vivo"

In the article referenced above [Kunze KL, Nelson WL, Kharasch EV, Thummel KE, and Isoherranen N (2006), *Drug Metab Dispos* **34:**583-590; doi:10.1124/dmd.105.008508], the stereochemical assignments of itraconazole and metabolite stereoisomers in Figs. 1 and 2 were incorrect. The corrected assignments and revised Figs. 1 and 2 are provided below. This error does not affect the identification of metabolized stereoisomers or the in vivo pharmacokinetic analysis in the manuscript. The error was solely in the figure labels.

The authors regret this error and any confusion it may have caused.

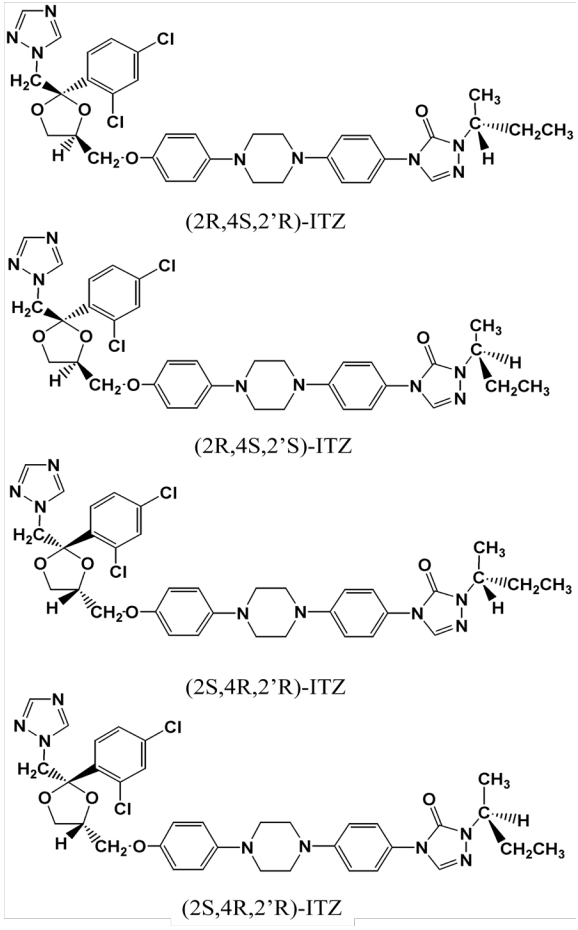

Fig. 1. Structures of the four stereoisomers of itraconazole.

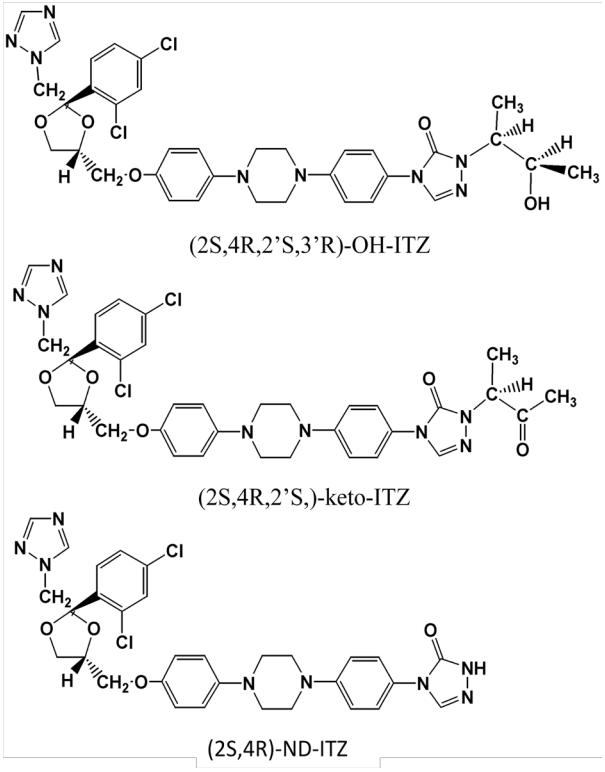

Fig. 2. Structures of the metabolites of itraconazole: OH-ITZ, keto-ITZ and ND-ITZ. Only one of the possible stereoisomers formed in vivo is depicted for each metabolite.